ELSEVIER

International Journal of Mass Spectrometry 225 (2003) 11–23

International Journal of Mass Spectrometry

www.elsevier.com/locate/ijms

The isobaric ions $CH_3O–P{=}O^{\bullet+}$ and $CH_3O–P–NH_2^+$ and their neutral counterparts: a tandem mass spectrometry and CBS-QB3 computational study

Lisa N. Heydorn[a], Cathy Y. Wong[a], R. Srinivas[b], Johan K. Terlouw[a,*]

[a] *Department of Chemistry, McMaster University, 1280 Main Street West, Hamilton, Ont., Canada L8S 4M1*
[b] *Indian Institute of Chemical Technology, Hyderabad 500 007, India*

Received 27 August 2002; accepted 26 September 2002

Abstract

In contrast to a previous report [J. Mass Spectrom. 171 (1997) 79], the dissociative electron ionization of acephate does not generate pure *m/z* 78 ions $CH_3O–P{=}O^{\bullet+}$. By combining the results of exact mass measurements, (multiple) high energy collision experiments and CBS-QB3 calculations, it is concluded that the *m/z* 78 ions consist of $CH_3O–P{=}O^{\bullet+}$ and $CH_2O–P–OH^{\bullet+}$ in admixture with isobaric CH_5PON^+ ions. A computational analysis of the dissociation characteristics of the independently generated stable isomers $CH_3O–P–NH_2^+$ and $CH_3P(=O)NH_2^+$ shows that the CH_5PON^+ ions from acephate have the structure $CH_3O–P–NH_2^+$. As a consequence, the recovery signal in the reported neutralization–reionization (NR) spectrum of acephate's *m/z* 78 ions does not prove the stability of the $CH_3O–P{=}O$ neutral. Definitive evidence for its existence as a stable species in the dilute gas phase comes from a collision-induced dissociative ionization (CIDI) experiment on the reaction $C_6H_5–P(=O)OCH_3^+ \rightarrow C_6H_5^+ + CH_3O–P{=}O$. The calculations indicate that $CH_3O–P–NH_2^{\bullet}$ is also a stable species, but attempts to confirm this by experiment have not yet been successful.

Keywords: Tandem mass spectrometry; Neutralization–reionization mass spectrometry; Ab initio calculations; CBS-QB3; Acephate (*O*,*S*-dimethyl acetylphosphoramidothioate); Methamidophos (*O*,*S*-dimethylphosphoramidothiolate)

1. Introduction

Neutralization–reionization mass spectrometry (NRMS) has been established as a powerful tool to probe the structure (atom connectivity) and stability of elusive and often highly reactive molecules or radicals in the rarefied gas phase (for selected recent reviews see [1]). However, the technique is not without its pitfalls, particularly when the NR experiment involves a weak secondary or tertiary fragment ion in the electron impact mass spectrum of a precursor molecule containing several heteroatoms. In such a case, it is important to check whether the beam of ions to be neutralized contains isobaric and/or isomeric impurities that may compromise the interpretation of the experimental findings. The NR efficiencies of a given set of isobaric or isomeric ions can differ by several orders of magnitude and thus the mere presence of a recovery signal in a NR spectrum does not necessarily attest to the stability of the neutral counterpart of the major ionic component of the

* Corresponding author. Tel.: +1-905-525-9140x27111; fax: +1-905-522-2509.
E-mail address: terlouwj@mcmaster.ca (J.K. Terlouw).

1387-3806/02/$ – see front matter
PII S1387-3806(02)01026-6

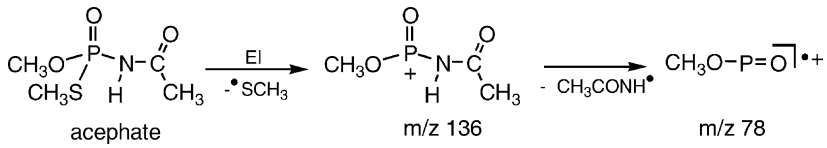

Scheme 1.

neutralized ion beam. The presence of isobaric impurities may be probed by a high resolution experiment but the isomeric purity of a given beam of ions is more difficult to establish. One approach involves selectively transmitting the beam of "survivor" ions represented by the recovery signal to a collision gas chamber to obtain its collision-induced dissociation (CID) spectrum [1b]. Comparison of the resulting CID/NR spectrum (which can only be obtained if the recovery signal is sufficiently intense) with the CID spectrum of the source generated ions provides important information on the purity of the initial ion beam. Such an experiment also addresses the question of whether the incipient neutral has retained its structure identity (for a recent example see [2]). For many systems of ions, a conclusive analysis of the NR results requires a detailed knowledge of the energy requirements of the potential isomerization and dissociation reactions of both the ion and its neutral counterpart. The use of state-of-the-art computational chemistry, particularly the Gaussian and CBS model chemistries [3], is indispensable in this context. An elegant example of the important role of computational chemistry is the recent NR study of the bicoordinated dihydroxyphosphenium ion, $P(OH)_2^+$ [4].

Many other O- and/or S-containing low coordinated phosphorus ions have been studied by the NR technique [4], including the *m/z* 78 ion $CH_3O–P{=}O^{\bullet+}$, (methoxy)oxo-phosphane [5]. The *m/z* 78 ions of this study were obtained by the dissociative ionization of the insecticide acephate [6], which was proposed to yield pure ions $CH_3O–P{=}O^{\bullet+}$ via the sequential losses of $CH_3S^{\bullet}$ and $CH_3C(=O)NH^{\bullet}$, as depicted in Scheme 1.

The CID spectrum of these *m/z* 78 ions displays a prominent peak at *m/z* 46, which was attributed to a rearrangement reaction involving the unusual loss of an O_2 molecule: $CH_3O–P{=}O^{\bullet+} \rightarrow CH_3P^{\bullet+}$ (m/z 46) + O_2. This interpretation seemed to be at odds with findings from our study of the intriguing decarbonylation reaction of some 10 key isomers of the family of $CH_3PO_2^{\bullet+}$ ions, including the $CH_3O–P{=}O^{\bullet+}$ ion [7]. Experiment and theory [7] (CBS-QB3 calculations, see Section 2) agree that $CH_3O–P{=}O^{\bullet+}$ can readily communicate with its more stable distonic isomer $CH_2O–P–OH^{\bullet+}$. The latter ion can readily be obtained by the dissociative ionization of ethylene phosphonate or ethylene phosphite [8]. Its CID spectrum is closely similar but not identical to that of the *m/z* 78 ions of putative structure $CH_3O–P{=}O^{\bullet+}$, which we had generated by the dissociative ionization of $CH_3O–P(=O)Br_2$ and $CH_3O–P(=O)Cl_2$. The spectra of the two isomers are dominated by peaks at *m/z* 31 (CH_2OH^+), 47 (PO^+), and 48 ($POH^{\bullet+}$) but a signal at *m/z* 46 was conspicuously absent. This prompted us to reexamine the structure and origin of the *m/z* 78 ions generated from acephate. The *m/z* 78 ions generated from its analogue methamidophos, $CH_3S(CH_3O)P(=O)NH_2$ (a hydrolysis product of acephate [6]) were also examined.

Results from exact mass measurements, (multiple) collision experiments, and CBS-QB3 calculations will be presented to show that the *m/z* 78 ions generated by acephate consist of the $CH_3PO_2^{\bullet+}$ isomers $CH_3O–P{=}O^{\bullet+}$ and $CH_2O–P–OH^{\bullet+}$, in admixture with the CH_5PON^+ isomer $CH_3O–P–NH_2^+$. For methamidophos, the latter ion is the principal component. Its NR spectrum displays an intense recovery signal. As a consequence, the recovery signal in the reported NR spectrum of acephate cannot be used to prove the stability of the $CH_3O–P{=}O$ neutral. Definitive evidence for its existence as a stable species in the gas phase comes from a collision-induced dissociative ionization (CIDI) [9] experiment on methyl phenylphosphinate, $C_6H_5–P(=O)(H)OCH_3$.

2. Experimental and theoretical methods

2.1. Sample preparation procedures

Acephate ($CH_3S(CH_3O)P(=O)N(H)C(=O)CH_3$, *O*, *S*-dimethyl acetylphosphoramidothioate) and methamidophos ($CH_3S(CH_3O)P(=O)NH_2$, *O*,*S*-dimethylphosphoramidothiolate), were of research grade and obtained from Sigma-Aldrich. The deuterium isotopologue $CH_3S(CH_3O)P(=O)ND_2$ was obtained by exchange of the acidic hydrogens with D_2O.

Methyl dichlorophosphate ($CH_3O–P(=O)Cl_2$) was obtained from Aldrich. A small sample of its thermally labile dibromo analogue was prepared as described in [10a]. The labeled isotopologues, $CH_3{}^*O–P(=O)Cl_2$ and $CD_3O–P(=O)Cl_2$ were synthesized by methanolysis of trichlorophosphate [10b]. Ethylene phosphonate (1,3,2-dioxaphospholane, 2-oxide) and ethyl ethylene phosphite were obtained as described in [8]. Methyl phenylphosphinate ($C_6H_5–P(=O)(H)OCH_3$) was obtained by the reaction of phenylphosphinic acid (Aldrich) with methylchloroformate [10b].

Methylphosphonamidic chloride ($CH_3P(=O)NH_2Cl$) was obtained from the reaction of two equivalents of gaseous ammonia with methylphosphonic dichloride (Aldrich) in diethylether, following the general procedure described in [10c,d].

2.2. Mass spectrometry

The Micromass GC-T time-of-flight mass spectrometer was used to obtain 70 eV EI mass spectra at its standard mass resolution of 4000–6000 (50% valley definition) at *m*/*z* 69 of the reference compound 2,4,6-tris(trifluoromethyl)-1,3,5-triazine. The spectra were obtained in the continuous mode which allows an off-line examination of the shape(s) of the signals at each and every nominal mass in the EI spectrum. In the assignment of an elemental composition, all combinations of C/H/N/O/P/S were considered whose calculated mass deviated by not more than 10 mDa from the measured mass. However, unless stated otherwise, the reported elemental compositions deviated by less than 1 mDa. The acephate and methamidophos samples were introduced via the solids probe in microgram quantities so as to obtain complete evaporation profiles. In these experiments the probe was kept at room temperature and the ion source at ca. 100 °C.

The tandem mass spectrometry-based experiments were performed with the VG Analytical ZAB-R mass spectrometer, a three-sector BE_1E_2 (B = magnetic sector, E = electric sector) type instrument [11].

The compounds were introduced into the ion source (kept at 100 °C) via either the solids probe or a wide-bore all-quartz direct insertion probe connected via an o-ring with a small glass bulb that contains the sample. Ions generated in the source by electron ionization (EI) were accelerated to 8 or 10 keV prior to recording their spontaneous or collision-induced dissociations in the second or the third field-free regions (ffr) as metastable ion (MI) or CID spectra, respectively. The structure of a given product ion in a 2ffr MI or CID spectrum was probed by selectively transmitting the ion by E_1 to a collision chamber in the 3ffr pressurized with O_2 and mass-analyzing its ionic dissociation products by scanning E_2. The resulting MS/MS/MS type spectra are denoted as MI/CID and CID/CID spectra, respectively. All the (high energy) collision experiments were performed at a main beam transmittance (∼70%) such that the probability for multiple collisions is negligible.

For NRMS [1], 8 keV ions $m^{\bullet+}$ are selectively transmitted by B to the 2ffr where, in the first collision chamber, charge-exchange neutralization occurs with *N*,*N*-dimethyl aniline (NDMA): $m^{\bullet+}[8\,keV] + NDMA \rightarrow m\,[8\,keV] + NDMA^{\bullet+}$. The unreacted ions are deflected away and the remaining fast neutrals are reionized with O_2 in the second collision cell. Scanning E_1 yields the spectrum of the reionized neutrals $m^{\bullet+}$, the "survivor" ions, and their (structure characteristic) charged dissociation products. For CIDI experiments [9], 10 keV ions are selectively transmitted by B to the 2ffr where the metastable ions spontaneously dissociate. The ions are deflected away and the remaining low energy neutrals, which have a fraction of the original 10 keV translational energy, are reionized by O_2 in the second collision cell. The ionized neutrals and their dissociation products

are mass-analyzed by scanning with E_1. All spectra were recorded using a small PC-based data system developed by Mommers Technologies Inc. (Ottawa).

2.3. Computational procedures

Structures and energies of the $CH_3O_2P^{\bullet+}$ and CH_5NOP^+ isobaric ions pertinent to this study, connecting transition states and dissociation products were probed by the standard CBS-QB3 model chemistry [12]. A recent study [13] indicates that this method accurately reproduces the heats of formation of species comprised of a second row element (S or P) bonded to a highly electronegative element. The calculations were performed using Gaussian 98, Revision A.9 [14].

The calculated energies are presented in Table 1a (equilibrium and transition state energies) and Table 1b (dissociation products) while the complete set of detailed geometries is available upon request. Frequency calculations gave the correct number of negative eigenvalues for all minima and transition states and the spin contamination was within the acceptable range. The connections of the transition states have been checked by geometry optimizations and frequency calculations.

Table 1a
CBS-QB3-derived heats of formation of selected $CH_3PO_2^{\bullet+}$ and CH_5PNO^+ isomeric ions, dissociation products and neutral counterparts

		E_{total}[a]	ZPVE	ΔH_f° (0 K)	ΔH_f° (298 K)	E_{rel} (298 K)
CH_3O–P=$O^{\bullet+}$ (*anti*)	**1a**$^{\bullet+}$	−530.68346	27.61	137.9	135.4	14
CH_2O–P–$OH^{\bullet+}$ (*syn*/*anti*)	**1b**$^{\bullet+}$	−530.70506	26.64	124.4	121.5	0
$CH_2O(H)$–P=$O^{\bullet+}$ (*syn*)	**1c**$^{\bullet+}$	−530.66664	25.60	148.5	146.5	25
$[CH_2$–$OH]^+ \cdots$ O=$P^{\bullet}$	**1d**$^{\bullet+}$	−530.69034	26.50	133.6	131.1	10
CH_2O–P(H)=$O^{\bullet+}$	**1e**$^{\bullet+}$	−530.67567	25.57	142.8	140.1	19
CH_3O–P=O (*anti*)	**1a**	−531.06246	28.14	−99.9	−102.7	
TS **1a**$^{\bullet+}$ → **1b**$^{\bullet+}$ (*syn*/*syn*)		−530.65170	27.70	160.0	156.8	35
TS **1b**$^{\bullet+}$ → **1d**$^{\bullet+}$		−530.67052	25.99	146.0	143.4	22
TS **1e**$^{\bullet+}$ → **1b**$^{\bullet+}$		−530.62551	23.58	174.3	171.6	50
TS **1a**$^{\bullet+}$ → **1c**$^{\bullet+}$		−530.60896	25.60	184.7	182.1	61
$CH_2OH^+ + PO^{\bullet}$	*m*/*z* 31				160.5	39
$POH^{\bullet+} + CH_2$=O	*m*/*z* 48				164.3	43
$PO^+ + CH_3O^{\bullet}$	*m*/*z* 47				188.8	67
CH_3O–P–NH_2^+	**2a**$^+$	−511.50023	42.91	116.4	111.4	3
CH_3–P(=O)–NH_2^+	**2b**$^+$	−511.50576	42.19	112.9	108.4	0
CH_3O–P(H)=NH^+	**2c**$^+$	−511.44197	41.01	152.9	148.0	40
$CH_3O(H)$–P=NH^+	**2d**$^+$	−511.45158	41.63	146.9	143.0	35
CH_2O–P(H)–NH_2^+	**2e**$^+$	−511.45918	41.02	142.1	137.9	30
TS **2a**$^+$ → **2c**$^+$		−511.37659	41.01	193.9	188.4	80
TS **2a**$^+$ → **2d**$^+$		−511.42402	39.56	164.2	159.5	51
TS **2a**$^+$ → **2e**$^+$		−511.41573	41.02	169.4	164.5	56
$HNP^+ + CH_3OH$	*m*/*z* 46				168.4	60
$H_2NP^{\bullet+} + CH_3O^{\bullet}$	*m*/*z* 47				223.3	115
$PO^+ + CH_3NH_2$	*m*/*z* 47				179.7	71
$H_2NPH^+ + CH_2$=O	*m*/*z* 48				164.1	56
$NH_2PO^{\bullet+} + CH_3^{\bullet}$	*m*/*z* 63				212.8	104
$CH_3OP^{\bullet+} + NH_2^{\bullet}$	*m*/*z* 62				230.4	122
CH_3O–P–$NH_2^{\bullet}$	**2a**$^{\bullet}$	−511.72871	40.79	−27.0	−31.6	20
CH_3–P(=O)–$NH_2^{\bullet}$	**2b**$^{\bullet}$	−511.76172	41.22	−47.7	−52.1	0
CH_3O–P(H)–$NH^{\bullet}$	**2c**$^{\bullet}$	−511.70356	39.99	−11.2	−15.6	36

[a] E_{total} is given in Hartrees, all other components, including the ZPVE scaled by 0.99, are in kcal/mol.

Table 1b
Auxiliary energetic information derived from CBS-QB3 calculations

	m/z	E_{total}[a]	ZPVE	ΔH_f° (0 K)	ΔH_f° (298 K)
NH_2–P(OH)$OCH_3^{\bullet+}$	95	−587.24443	51.63	65.9	60.5
NH_2–P(H)(=O)$OCH_3^{\bullet+}$	95	−587.19634	50.42	96.0	90.6
NH_3–P(=O)OCH_2^+	94	−586.64345	44.56	77.7	73.5
NH_2–P(=O)$OCH_3^{\bullet+}$	94	−586.66456	45.98	64.5	59.5
NH_2–P(OH)OCH_2^+	94	−586.65380	43.91	71.2	66.8
H–N=P=S^+	78	−793.59210	8.95	244.2	242.9
CH_3–P=$S^{\bullet+}$	78	−778.15710	23.03	216.4	213.8
HO–P=$O^{\bullet+}$	64	−491.45052	10.15	145.7	144.3
PO_2^+	63	−415.72469	4.15	176.7	176.0
$PO_2^\bullet$		−491.21376	2.60	−71.0	−71.7
PS^+	63	−738.34694	1.20	219.0	218.8
NH_2–P=$O^{\bullet+}$	63	−471.59670	18.03	179.7	177.3
$CH_3OP^{\bullet+}$	62	−455.52242	25.65	187.7	185.4
H–N=P=O^+	62	−470.94968	9.72	220.4	219.1
H_2N–PH_3^+	50	−398.28525	33.43	164.7	160.4
H–P–NH_2^+	48	−397.07402	22.09	194.2	191.4
H–P=$O^{\bullet+}$	48	−416.25538	5.15	217.0	216.1
P–$OH^{\bullet+}$	48	−416.29431	7.62	192.5	191.6
P–$NH_2^{\bullet+}$	47	−396.44950	15.69	220.9	219.0
H–N=P–$H^{\bullet+}$	47	−396.40210	12.38	250.6	248.9
PO^+	47	−416.27365	2.03	184.7	184.5
$PO^\bullet$		−416.03233	1.75	−8.4	−8.6
CH_2=$PH^{\bullet+}$	46	−380.32624	19.54	259.6	257.7
CH_3–$P^{\bullet+}$	46	−380.33435	20.46	254.5	252.7
N=P–H^+	46	−395.73221	5.08	305.7	304.7
H–N=P^+	46	−395.87172	8.07	218.1	217.3
CH_3OH		−115.53992	31.44	−46.2	−48.9
CH_2OH^+	31	−114.61170	24.94	171.0	169.1
$CH_3O^\bullet$		−114.87446	22.45	6.1	4.3
CH_3NH_2		−95.66848	39.24	−1.2	−4.8
CH_2=O		−113.94253	16.29	−26.4	−27.3
H_2O		−76.33746	13.11	−57.5	−58.2
O		−74.98763	0.00	59.0	59.4
$NH_2^\bullet$		−55.79118	11.61	45.7	45.0
CH_3^+	15	−39.38466	19.17	262.2	261.3
$CH_3^\bullet$		−39.74479	18.19	36.6	35.5

[a] E_{total} is given in Hartrees, all other components, including the ZPVE scaled by 0.99, are in kcal/mol.

3. Results and discussion

3.1. The elemental composition of the m/z 78 ions from acephate and methamidophos

The 70 eV EI mass spectra of acephate and methamidophos are presented in Fig. 1, as items (a) and (b), respectively. These spectra were obtained with the ZAB-R instrument. They are virtually the same as those from the GC-TOF instrument and closely similar to the spectra reported in the literature [16]. It is seen from Fig. 1a and b that the *m/z* 78 ions are of only minor abundance and, considering the structure of the precursor molecules, they are obviously not primary fragment ions. From our analysis of the MI and CID spectra (Section 3.3), it follows that the *m/z* 78 ions from acephate have four precursor ions, viz. *m/z* 136, 96, 95 and 94. For methamidophos *m/z* 78 ions appear in the CID spectra of *m/z* 95 and 94.

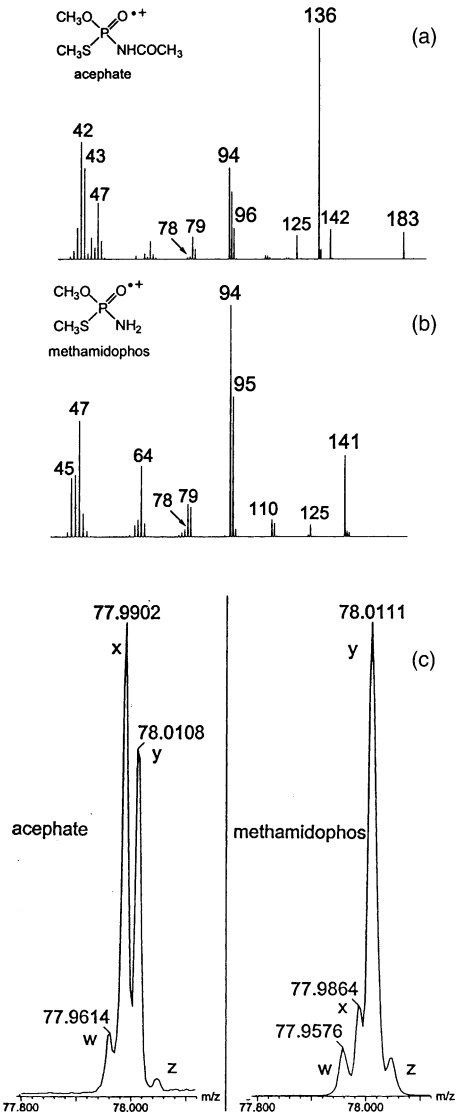

Fig. 1. The 70 eV EI mass spectra of acephate (a) and methamidophos (b); (c) displays the *m/z* 78 peak profiles for the two compounds obtained at medium mass resolution, see text for further details.

Fig. 1c shows a narrow mass scan of the *m/z* 78 ions from the two precursor molecules obtained with a GC-TOF instrument at a mass resolution of ca. 5000. Both acephate and methamidophos yield a mixture of four isobaric ions whose common components are denoted as *w*, *x*, *y* and *z*. The relative intensity of the *x*, *y* and *w* components remains constant during the evaporation of the sample, but that of the *z* component decreases steadily. This *z* component of centroid mass 78.0458 most likely stems from a minor benzene impurity of the samples: it is not present when the sample was analyzed in the GC/MS mode.

The ions derived from acephate consist of two major components, *x* and *y*. Their centroid masses, 77.9870 and 78.0104, agree with the elemental compositions CH_3O_2P and CH_5NOP, whose calculated masses differ from the measured masses by 0.0 and 0.4 mDa. For methamidophos, the CH_5NOP component (*y*) clearly dominates. The minor *w* component could refer to the PS containing ions HNPS and/or CH_3PS.

The *m/z* 94 precursor ions are isobarically pure $CH_5NO_2P^+$ ions; the *m/z* 95 $CH_6NO_2P^{\bullet+}$ ions from methamidophos are also isobarically pure, but those from acephate consist of a 5:1 mixture of $CH_6NO_2P^{\bullet+}$ and $CH_4O_3P^+$. The *m/z* 136 $C_3H_7NO_3^+$ and *m/z* 96 $CH_5O_3P^{\bullet+}$ ions from acephate both have a single elemental composition.

Thus, unlike the proposal of [5], the *m/z* 78 ions of acephate are not isobarically pure ions $CH_3O–P{=}O^{\bullet+}$. The minor PS containing component may have little impact on the CID spectrum, but the major CH_5NOP^+ component will certainly contribute. The analysis of the NR spectrum becomes even more problematic. To facilitate the analysis of the CID and NR spectra in Section 3.4, we will first discuss the characterization of isobarically pure $CH_3O–P{=}O^{\bullet+}$ ions and their neutral counterpart.

3.2. The dissociation characteristics of $CH_3O–P{=}O^{\bullet+}$ and its H-shift isomer $CH_2O–P–OH^{\bullet+}$

As mentioned above, we have studied the $CH_3O_2P^{\bullet+}$ system of isomers in considerable detail [7]. In the context of the present study we will focus on the collision-induced dissociation characteristics of $CH_3O–P{=}O^{\bullet+}$, **1a**$^{\bullet+}$, and its H-shift isomer $CH_2O–P–OH^{\bullet+}$, **1b**$^{\bullet+}$. The ions are generated as depicted in Scheme 2 and their CID spectra are presented in Fig. 2.

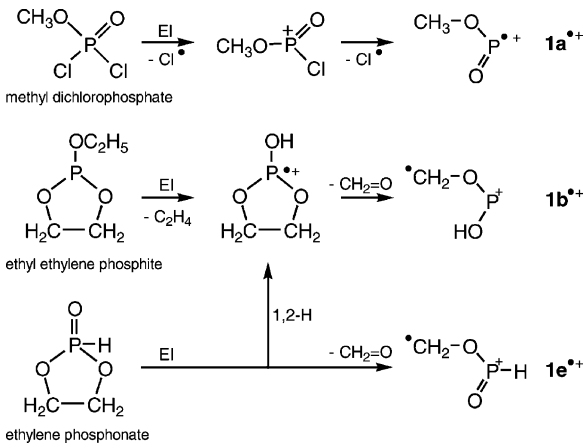

Scheme 2.

Comparison of the spectra indicates that the major collision-induced dissociations of the two isomers lead to the same product ions, viz. CH_2OH^+ (*m/z* 31), PO^+ (*m/z* 47) and $POH^{\bullet+}$ (*m/z* 48). From the results presented in Tables 1a and b, it follows that the minimum energy requirement for dissociation into $CH_2OH^+ + PO^\bullet$ is lower than that for the formation of $PO^+ + CH_3O^\bullet$ and $POH^{\bullet+} + CH_2{=}O$, by 28 and 4 kcal/mol, respectively. The dissociation $CH_2OH^+ + PO^\bullet$ is also observed for metastable ions **1a**$^{\bullet+}$ and **1b**$^{\bullet+}$—along with a prominent decarbonylation into *m/z* 50 $HPOH_2^{\bullet+}$ ions [7]—but peaks at *m/z* 48 and 47 are absent in the MI spectra (not shown). The *m/z* 48 $POH^{\bullet+}$ ion can be generated from $CH_2O{-}P{-}OH^{\bullet+}$, **1b**$^{\bullet+}$, by direct bond cleavage and the same holds true for the formation of PO^+ (*m/z* 47) from $CH_3O{-}P{=}O^{\bullet+}$, **1a**$^{\bullet+}$. However, the formation of CH_2OH^+ from either of the isomers requires a H-shift. Our computational results (see Tables 1a and b), show that the 1,4-H shift associated with the interconversion of **1a**$^{\bullet+}$ and **1b**$^{\bullet+}$ is less energy demanding than the major CID dissociations. Moreover, ions **1b**$^{\bullet+}$ can rearrange via a low barrier into the hydrogen-bridged radical cation $^+CH_2{-}O{-}H\cdots O{=}P^\bullet$, **1d**$^{\bullet+}$, which may serve as a precursor for the formation of CH_2OH^+. At more elevated energies, CH_2OH^+ ions may also be generated via the sequence **1a**$^{\bullet+}$—1,2-H → $CH_2O(H){-}P{=}O^{\bullet+}$, **1c**$^{\bullet+}$ → $CH_2OH^+ + P{=}O^\bullet$ (see Tables 1a and b). Thus, it is not surprising that the CID spectrum of **1a**$^{\bullet+}$ is similar to that of its more stable distonic isomer **1b**$^{\bullet+}$. This is also true for the CID spectrum of another high energy H-shift isomer of **1b**$^{\bullet+}$, $CH_2OP(H){=}O^{\bullet+}$, **1e**$^{\bullet+}$, which is co-generated with **1b**$^{\bullet+}$ upon the loss of CH_2O from ionized ethylene phosphonate (see Scheme 2) [7].

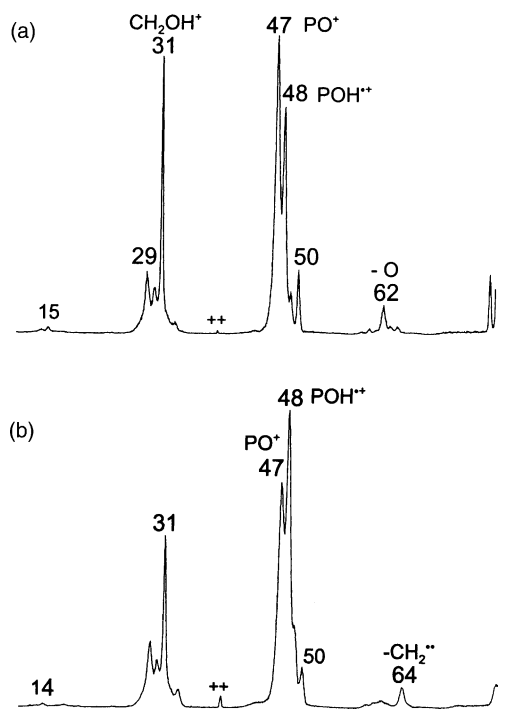

Fig. 2. The 8 keV CID mass spectra (3ffr) of the *m/z* 78 CH_3PO_2 isomers $CH_3O{-}P{=}O^{\bullet+}$, spectrum (a), and $CH_2O{-}P{-}OH^{\bullet+}$, spectrum (b).

Nevertheless, isomers **1a**$^{\bullet+}$ and **1b**$^{\bullet+}$ can be differentiated on the basis of the weak but structure diagnostic CID peaks at *m/z* 62 and 64. These peaks represent high energy dissociations, viz. $CH_3O{-}P{=}O^{\bullet+}$ → $CH_3OP^{\bullet+}(m/z\,64) + O$ and $CH_2O{-}P{-}OH^{\bullet+}$ → $HO{-}P{=}O^{\bullet+} + CH_2^{\bullet\bullet}$. The loss of O from **1a**$^{\bullet+}$ is less pronounced when helium is used as a collision gas rather than O_2, in line with the "oxygen effect" described in [17]. Finally, in line with the expected stability of dications **1b**$^{++}$ vs. **1a**$^{++}$, the distonic ion **1b**$^{\bullet+}$ displays a more pronounced *m/z* 39 charge stripping peak in its CID spectrum.

One further point deserves comment: in the CID spectrum of the *m/z* 78 ions of putative structure **1a**$^{\bullet+}$ derived from acephate [5], a prominent peak is present at *m/z* 63 (see also Section 3.4). This peak has been assigned to the dissociation $CH_3O–P{=}O^{\bullet+} \rightarrow PO_2^+ (m/z\,63) + CH_3^\bullet$. Since $\Sigma\Delta H_f\, PO_2^\bullet + CH_3^+$ is lower than $\Sigma\Delta H_f\, PO_2^+ + CH_3^\bullet$, by 22 kcal/mol, the charge is expected to be retained at the methyl moiety upon cleavage of the C–O bond in **1a**$^{\bullet+}$. However, the intensity of the *m/z* 15 CH_3^+ peak in the reported spectrum [5] is negligible indicating that a prominent peak at *m/z* 63 does not characterize the CID spectrum of **1a**$^{\bullet+}$. On the other hand, in our spectrum of **1a**$^{\bullet+}$ presented in Fig. 2a, both *m/z* 15 and 63 are minor peaks. This is readily understood considering the ease of isomerization of $CH_3O–P{=}O^{\bullet+}$ upon collisional activation.

3.3. Evidence for the stability of the $CH_3O–P{=}O$ molecule in the rarefied gas-phase

As discussed above, $CH_3O–P{=}O^{\bullet+}$ ions yield a structure characteristic CID spectrum, albeit that the ion undergoes a facile interconversion with other H-shift isomers and is generated in a low yield. This makes it less attractive to probe the stability of the neutral by a NR experiment. We have therefore utilized a CIDI experiment, where the neutral of interest is generated by the dissociation of a selected metastable precursor ion and analyzed by its collisional ionization spectrum.

Loss of H$^\bullet$ dominates the 70 eV EI mass spectrum of methyl phenylphosphinate. The resulting even electron ion, $C_6H_5–P(=O)OCH_3^+$, yields the MI spectrum displayed in Fig. 3a. The spectrum shows that low energy ions $C_6H_5–P(=O)OCH_3^+$ undergo four dissociations. The peaks at *m/z* 125, 108 and 91 represent rearrangement reactions in which neutral species of 30, 47 and 64 Da are lost, most likely $CH_2{=}O$, PO$^\bullet$ and HPO_2, respectively. The MI spectrum also features the process of interest, the putative direct bond cleavage reaction $155^+ \rightarrow 77^+(C_6H_5^+) + 78$ ($CH_3O–P{=}O$). The alternative *rearrangement* reaction $155^+ \rightarrow 77^+(CH_2O–P{=}O^+) + 78$ (C_6H_6) has a lower calculated minimum energy requirement, by 26 kcal/mol (from the enthalpy values in Tables 1a and b and [15]). However, this rearrangement reaction must have a significant reverse activation energy since a collision experiment showed that most of the *m/z* 77 ions are $C_6H_5^+$. In the same vein, the prominent *m/z* 77 peak in the CID

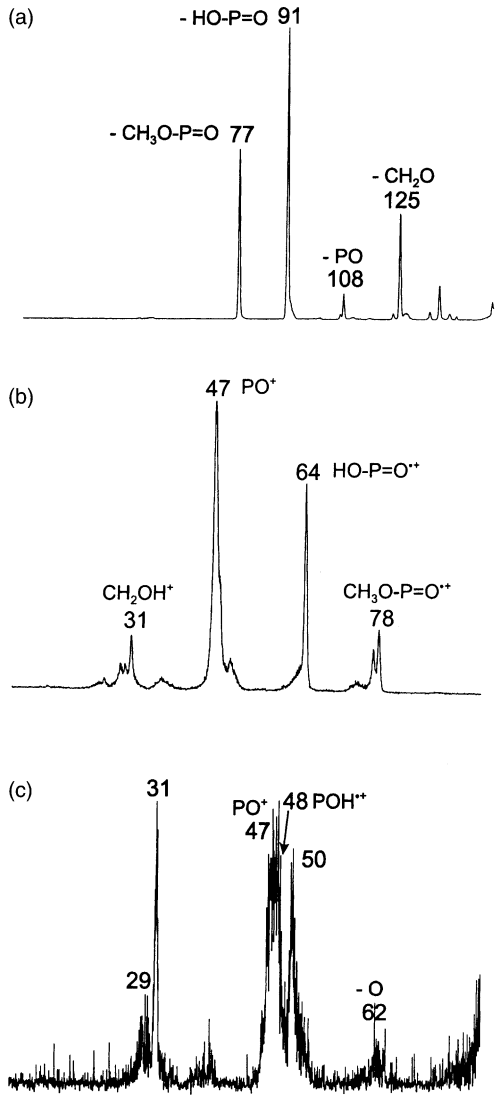

Fig. 3. The 10 keV MI and CIDI spectra of *m/z* 155 ions $C_6H_5–P(=O)OCH_3^+$, spectra (a) and (b), respectively; spectrum (c) is the 3ffr CID spectrum of the *m/z* peak of spectrum (b).

spectrum of C_6H_5–P(=O)OCH_3^+ also refers to $C_6H_5^+$ ions.

In the CIDI experiment the beam of mass selected *m/z* 155 ions, which also contains its ionic dissociation products, is deflected away by an electrode in front of the collision gas chamber. Thus, ideally the only species that enter this chamber are the four neutral species generated from the above reactions. These neutrals are subsequently ionized by collision (albeit with considerably different efficiencies which depend on the translational energy and other factors [18]) and the resulting ions and their ionic dissociation products give rise to the CIDI spectrum of Fig. 3b. The spectrum shows a sizable peak at *m/z* 78, expected to correspond to collisional ionization of CH_3O–P=O. That this is indeed the case follows from Fig. 3c which presents the CID spectrum of the *m/z* 78 ions of Fig. 3b. Although the weak spectrum suffers from a fairly high noise level, there is little doubt that we are dealing with ions of structure **1a**$^{\bullet+}$.

Thus, we conclude that CH_3O–P=O is a stable molecule in the gas phase, in agreement with our CBS-QB3 calculations from which we derive ΔH_f^{298} [**1a**] = −102.7 kcal/mol and IE_a [**1a**] = 10.3 eV (see Tables 1a and b).

Two points deserve further comment: (i) the NR spectrum (not shown) of the *m/z* 155 C_6H_5–P(=O)OCH_3^+ ions displays a prominent *m/z* 77 ($C_6H_5^+$) peak with only minor peaks at higher masses. In a CIDI experiment with O_2 for collisional ionization, the gas pressure in the region immediately in front of the deflector electrode is often sufficiently high to cause some neutralization of the beam of incoming ions [9b]. This phenomenon, we propose, accounts for the presence of the peak at *m/z* 77 in the CIDI spectrum of Fig. 3b; (ii) as mentioned above, decarbonlylation into *m/z* 50 ions is the major reaction of metastable CH_3O–P=O$^{\bullet+}$ ions. In line with the general observation that ions generated by collisional ionization contain a higher fraction of metastable ions than those generated by electron impact in the ion source [19], the relative intensity of the *m/z* 50 peak in Fig. 3c is higher than that of Fig. 2a.

3.4. The collision-induced dissociation characteristics of m/z 78 ions from acephate and methamidophos: evidence for the generation of the CH_3O–P–NH_2^+ ion

Fig. 4a displays the CID spectrum of the source generated *m/z* 78 ions derived from acephate which (see Section 3.1), consist of roughly a 1:1 mixture of $CH_3PO_2^{\bullet+}$ and CH_5NOP^+ ions with a small contribution from $HNPS^+$ and/or $CH_3PS^{\bullet+}$. Comparison of the spectrum with that of CH_3O–P=O$^{\bullet+}$ (Fig. 2a), shows that the prominent *m/z* 46 peak does not originate from the $CH_3PO_2^{\bullet+}$ component but rather from the isobaric CH_5NOP^+ ions. This is supported by the enhanced intensity of the *m/z* 46 peak in the CID spectrum of Fig. 4d, which samples the source generated *m/z* 78 ions from methamidophos which largely consist of CH_5NOP^+ ions. Consequently, the proposal of [5] that the *m/z* 46 ions originate from the dissociation CH_3O–P=O$^{\bullet+}$ → $CH_3P^{\bullet+}$ (*m/z* 46) + O_2 is clearly not tenable. In fact, the relative high heat of formation of $CH_3P^{\bullet+}$ (Table 1b) makes it highly unlikely that this ion is generated to a significant extent from any $CH_3PO_2^{\bullet+}$ isomer.

To probe the structure(s) of the $CH_3PO_2^{\bullet+}$ and CH_5NOP^+ ions from acephate and methamidophos, we analyzed the CID spectra of all potential precursor ions.

For methamidophos, we found two routes: (i) M$^{\bullet+}$ → *m/z* 94 ($CH_5NO_2P^+$) + $CH_3S^{\bullet}$ and (ii) M$^{\bullet+}$ → *m/z* 95 ($CH_6NO_2P^{\bullet+}$) + CH_2=S. The intense *m/z* 94 ions (see Fig. 1), are most likely ions of structure CH_3O–P(=O)NH_2^+, generated by a direct bond cleavage reaction. This ion is lower in energy than its isomers CH_2O–P(=O)NH_3^+ and CH_2O–P(OH)NH_2^+ (Table 1b) which could conceivably be generated from rearranged molecular ions. The prominent *m/z* 95 ions are most likely CH_3O–P(OH)$NH_2^{\bullet+}$ generated by loss of CH_2=S from molecular ions that have rearranged via a facile 1,4-H shift [13] into distonic ions CH_3O–P^+(OH)$(NH_2)SCH_2^{\bullet}$.

Ions at *m/z* 94 and 95 are also present in the EI mass spectrum of acephate. The ions have the same elemental composition as those derived from methamidophos

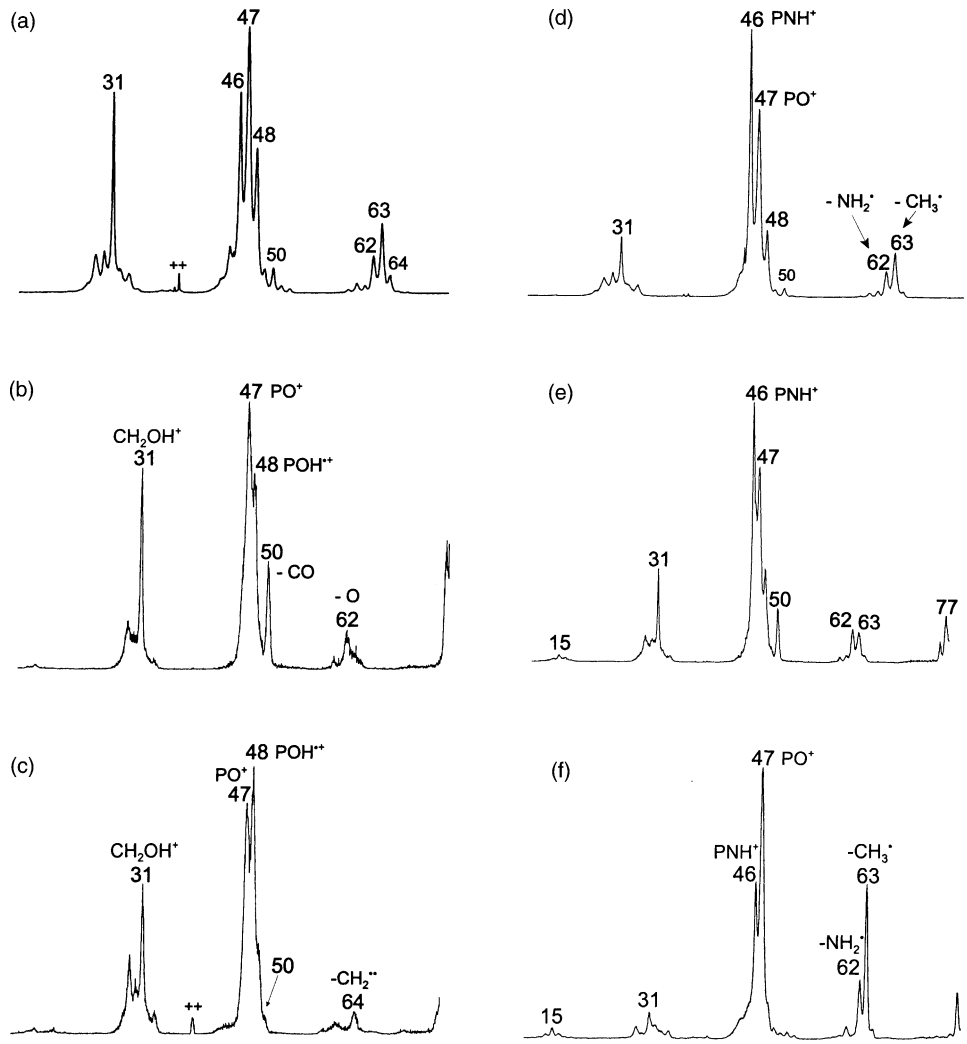

Fig. 4. The 8 keV CID mass spectra (3ffr) of *m/z* 78 ions: spectra (a and d) represent the source generated ions from acephate and methamidophos, respectively; spectra (b and c) are derived from the CID processes $136^+ \rightarrow 78^{\bullet+}$ and $96^{\bullet+} \rightarrow 78^{\bullet+}$ in acephate; spectrum (e) is derived from the CID process $94^+ \rightarrow 78^{\bullet+}$ in acephate/methamidophos; spectrum (f) refers to source generated ions of structure $CH_3P(=O)NH_2^+$.

(apart from a minor $CH_4O_3P^+$ component in *m/z* 95). Their CID spectra were obtained and found to be closely similar to those of the methamidophos-derived *m/z* 94 and 95 ions, signifying that we are dealing with ions of the same structure, i.e., $CH_3O–P(=O)NH_2^+$ and $CH_3O–P(OH)NH_2^{\bullet+}$, respectively. For acephate, the immediate precursor for both ions is the *m/z* 136 ion, but its CID spectrum indicates that a third route to *m/z* 78 may involve the direct bond cleavage reaction depicted in Scheme 1. The *m/z* 96 ion $CH_5O_3P^{\bullet+}$ in acephate's EI mass spectrum provides the fourth precursor to *m/z* 78. This ion is generated via the sequence $M^{\bullet+} \rightarrow m/z\,142 + C_2H_3N \rightarrow m/z\,96 + CH_2{=}S$, which represents a remarkable skeletal rearrangement. The MI spectrum of the *m/z* 96 ion shows intense peaks at *m/z* 78 (loss of H_2O) and *m/z* 66 (loss of CH_2O).

These peaks are also prominent in its CID spectrum, along with peaks at *m/z* 81 (loss of $CH_3^{\bullet}$) and *m/z* 65 (loss of $CH_3O^{\bullet}$), which support the proposal that the *m/z* 96 ions have the structure $CH_3O–P(OH)_2^{\bullet+}$.

For acephate, the CID spectra of the *m/z* 78 ions generated upon CID of the *m/z* 136 (route 3) and *m/z* 96 (route 4) ions are shown in Fig. 4b and c, respectively. The MS/MS/MS spectrum of Fig. 4b is very close to that of Fig. 2a, supporting the mechanistic proposal of Scheme 1, which leads to the formation of $CH_3PO_2^{\bullet+}$ ions of structure $CH_3O–P{=}O^{\bullet+}$. On the other hand, the spectrum of Fig. 4c is clearly not that of $CH_3O–P{=}O^{\bullet+}$ but rather that of $CH_2O–P–OH^{\bullet+}$, compare Fig. 2b. This is not unexpected: if the *m/z* 96 ion has the proposed structure $CH_3O–P(OH)_2^{\bullet+}$, a 1,4-H shift leading to the energetically more favorable distonic ion $CH_2O–P–OH^{\bullet+}$ is expected to be favored over a 1,3-H shift leading to $CH_3O–P{=}O^{\bullet+}$. From this analysis, it follows that the acephate molecular ion generates *m/z* 78 $CH_3PO_2^{\bullet+}$ ions which are a mixture of the isomers $CH_3O–P{=}O^{\bullet+}$ and $CH_2O–P–OH^{\bullet+}$.

We now turn to the structure and dissociation characteristics of the CH_5NOP^+ component, which dominates the CID spectrum of the source generated *m/z* 78 ions from methamidophos, Fig. 4d. From a comparison with the $CH_3PO_2^{\bullet+}$ reference spectra of Fig. 2, it becomes clear that the peaks at *m/z* 63 and particularly *m/z* 46 are tell-tale peaks of the CH_5NOP^+ ion. Assuming that the *m/z* 50 peak uniquely characterizes the isobaric $CH_3PO_2^{\bullet+}$ ions $\mathbf{1a}^{\bullet+}$ and $\mathbf{1b}^{\bullet+}$ (see Fig. 2), it further follows that most of the *m/z* 62 and a considerable fraction of the *m/z* 47 ions also originate from CH_5NOP^+. The MI spectrum (not shown) of the *m/z* 78 ions from methamidophos displays peaks at *m/z* 46, 48 and 50, with an intensity ratio of 100:35:25. The *m/z* 46 and 48 peaks characterize the low energy dissociations of the CH_5NOP^+ component since the $CH_3PO_2^{\bullet+}$ isomers do not display peaks at these *m/z* values in their MI spectra [7].

The CH_5NOP^+ ions from methamidophos may well have the structure $CH_3O–P–NH_2^+$, $\mathbf{2a}^+$, considering that there immediate precursor ions, *m/z* 94 and 95, can generate ions $\mathbf{2a}^+$ via direct bond cleavage reactions: $CH_3O–P(=O)NH_2^+$ (m/z 94) → $CH_3O–P–NH_2^+ + O$ and $CH_3O–P(OH)NH_2^{\bullet+}$ (m/z 95) → $CH_3O–P–NH_2^+ + OH^{\bullet}$. In support of this, our calculations (Table 1a) indicate that ion $\mathbf{2a}^+$ is a minimum on the CH_5NOP^+ potential energy surface. Its energy is comparable to that of its methyl-shift isomer $CH_3–P(=O)–NH_2^+$, $\mathbf{2b}^+$, but considerably lower than that of its H-shift isomers $CH_3O–P(H){=}NH^+$, $\mathbf{2c}^+$, $CH_3O(H)–P{=}NH^+$, $\mathbf{2d}^+$, and $CH_2O–P(H)–NH_2^+$, $\mathbf{2e}^+$. The methyl-shift isomer $\mathbf{2b}^+$ can conveniently be generated by loss of $Cl^{\bullet}$ from ionized $CH_3–(Cl)P(=O)–NH_2$ and its CID spectrum (see Fig. 4f), is clearly different from that of its isomer $\mathbf{2a}^+$ (Fig. 4d). We note that precursor molecules of the type $CH_3O–P(X)–NH_2$ (X = Cl, Br, CH_3O) [10d] which could abundantly yield isobarically pure ions $\mathbf{2a}^+$ upon ionization, are not known to exist.

The next step of our analysis is the CID spectrum of the *m/z* 78 ions generated by the collision-induced dissociation of the *m/z* 94 ions $CH_3O–P(=O)NH_2^+$, which is presented in Fig. 4e. The spectrum supports our proposal that CH_5NOP^+ ions of structure $\mathbf{2a}^+$ are generated. However, the peak at *m/z* 50 suggests that isobaric ions $\mathbf{1a}^{\bullet+}$, generated by the collision-induced dissociation $CH_3O–P(=O)NH_2^+$ (m/z 94) → $CH_3O–P{=}O^{\bullet+} + NH_2^{\bullet}$, are also present. The co-generation of $CH_3O–P{=}O^{\bullet+}$ also involves a direct bond cleavage reaction, but its minimum energy requirement is higher than that for dissociation into $\mathbf{2a}^+ + O$, by 9 kcal/mol (Table 1b). These dissociations are high energy processes and the intensity of the *m/z* 78 peak in the CID spectrum of *m/z* 94 is therefore only ca. 10% of the base peak at *m/z* 47 (PO^+). The *m/z* 78 peak in the CID spectrum of *m/z* 95 is even weaker and in addition it is poorly resolved from the base peak at *m/z* 79 ($CH_3O–P–OH^+$) which compromises a straightforward analysis. Nevertheless, the CID spectrum of the *m/z* 78 ions (not shown) resembles that of Fig. 4e and it is in basic agreement with the structure proposal.

Next, we analyzed the CID spectrum of the *m/z* 96 ion $CH_3O–P(=O)ND_2^+$, a D-labeled isotopologue of the *m/z* 94 ion $CH_3O–P(=O)NH_2^+$, obtained from methamidophos–ND_2. The spectrum shows peaks at *m/z* 80 and 78, in a 4:1 ratio, supporting the proposal

that the spectrum of Fig. 4e is a mixture of ions $\mathbf{2a}^+$ and $\mathbf{1a}^{\bullet+}$. The CID spectrum of the *m/z* 80 ions, which should be that of isobarically pure ions $CH_3O–P–ND_2^+$, has only three peaks in the *m/z* 45 region, viz. *m/z* 47 (100%, base peak), *m/z* 49 (25%) and *m/z* 50 (10%). In the *m/z* 60 region only two peaks are observed: at *m/z* 65 and 62, with an intensity ratio of 2:1. These observations allow us to identify the processes that give rise to the tell-tale peaks at *m/z* 46 and 63 in the CID spectrum of Fig. 4d as $\mathbf{2a}^+ \rightarrow HNP^+ + CH_3OH$ and $\mathbf{2a}^+ \rightarrow NH_2P{=}O^{\bullet+} + CH_3^\bullet$. The peak at *m/z* 62 may be assigned to the reaction $\mathbf{2a}^+ \rightarrow CH_3OP^{\bullet+} + NH_2^\bullet$, whereas the majority of the *m/z* 47 ions do not originate from the direct bond cleavage reaction $\mathbf{2a}^+ \rightarrow NH_2P^{\bullet+} + CH_3O^\bullet$ but rather result from the (formal) extrusion process: $\mathbf{2a}^+ \rightarrow PO^+ + CH_3NH_2$. We further note that the *m/z* 50 ions in the labeled isotopomer are most likely *m/z* 48 ions that contain two deuterium atoms, indicating that they are ions $HPNH_2^+$ generated by the rearrangement $\mathbf{2a}^+ \rightarrow HPNH_2^+ + CH_2O$.

Our computational results (see Table 1a), agree with this analysis. Ion $CH_3O–P–NH_2^+$ can undergo a 1,3-H shift (TS $\mathbf{2a}^+ \rightarrow \mathbf{2d}^+$) to yield ion $CH_3O(H)–P{=}NH^+$, $\mathbf{2d}^+$, which, by direct bond cleavage, yields $HNP^+ + CH_3OH$. Another 1,3-H shift (TS $\mathbf{2a}^+ \rightarrow \mathbf{2e}^+$) converts $\mathbf{2a}^+$ into $CH_2O–P(H)–NH_2^+$, $\mathbf{2e}^+$, which can lose CH_2O by direct bond cleavage to yield the *m/z* 48 ion H_2NPH^+. The two processes have comparable energy requirements, 60 and 56 kcal/mol, respectively, and are much lower in energy than all other processes observed. This is in line with the observation that *m/z* 46 and 48 characterize the MI spectrum of $\mathbf{2a}^+$. The activation energy of the direct bond cleavage $\mathbf{2a}^+ \rightarrow NH_2P^{\bullet+}$ (*m/z* 47) + $CH_3O^\bullet$ is very high (116 kcal/mol, Table 1a). It even exceeds that for $\mathbf{2a}^+ \rightarrow NH_2–P{=}O^{\bullet+}$ (*m/z* 63) + $CH_3^\bullet$, yet the *m/z* 47 CID peak is considerably more intense than *m/z* 63. Formation of isomeric *m/z* 47 ions $H–N{=}P–H^{\bullet+}$, via a 1,2-H shift into $CH_3O–P(H){=}NH^+$, $\mathbf{2d}^+$, followed by direct bond cleavage, requires even more energy: 146 kcal/mol. In contrast, the calculated minimum energy requirement is only 71 kcal/mol if, as proposed above, the *m/z* 47 ions are ions PO^+ generated from the reaction $\mathbf{2a}^+ \rightarrow PO^+ + CH_3NH_2$. In the same vein, the *m/z* 47 ions in the CID spectrum of the methyl-shift isomer $\mathbf{2b}^+$ may also be PO^+. Their generation can be envisaged as a simple extrusion reaction: $CH_3–P(=O)–NH_2^+ \rightarrow PO^+ + CH_3NH_2$, but the actual mechanism of this intriguing reaction may be more complex.

Thus, we conclude that the CH_5NOP^+ ions from methamidophos and acephate have the structure $CH_3O–P–NH_2^+$, $\mathbf{2a}^+$. Its neutral counterpart, $CH_3O–P–NH_2^\bullet$, **2a**, is calculated to be a stable species (see Table 1a), but confirmation of this prediction by a NR experiment on the *m/z* 78 ions from methamidophos appears to be problematic. The CID spectrum of the fairly abundant survivor ion of the NR process contains major peaks at *m/z* 63, 47, 46, 45 and 44, whose intensity distribution (100:70:90:85:35) is certainly not compatible with that of (pure) ions $\mathbf{2a}^+$. One speculative possibility is that the survivor ions are largely ions $CH_3PS^{\bullet+}/CH_3SP^{\bullet+}$, which could originate from the minor low mass *m/z* 78 component of methamidophos and acephate. Loss of $CH_3^\bullet$ is calculated to be an energetically favored dissociation for these ions, which could also account for the prominent peaks at *m/z* 45 (HCS^+) and *m/z* 44 ($CS^{\bullet+}$). In any case, these observations reinforce our conclusion that the NR spectrum of the *m/z* 78 ions from acephate reported in [5] cannot be used to verify by experiment that $CH_3O–P{=}O$ is a stable species in the gas-phase.

Acknowledgements

J.K.T. thanks the Natural Sciences and Engineering Research Council of Canada (NSERC) for continuing financial support. L.N.H. is grateful for the support provided by the Sherman Award and the Micromass-Canada Graduate Student Award. Discussions with Dr. P.C. Burgers and Professor P.J.A. Ruttink are gratefully acknowledged. J.K.T. and L.N.H. would like to thank Dr. Peter Hancock (Micromass UK Limited) and Zahra Jama (McMaster University) for their assistance in obtaining the mass spectra with the GC-T instrument.

References

[1] (a) G. Schalley, G. Hornung, D. Schröder, H. Schwarz, Chem. Soc. Rev. 27 (1998) 91;
(b) N. Goldberg, H. Schwarz, Acc. Chem. Res. 27 (1994) 34.

[2] M.A. Trikoupis, P. Gerbaux, D.J. Lavorato, R. Flammang, J.K. Terlouw, Int. J. Mass Spectrom. 217 (2002) 1.

[3] D. Young, Computational Chemistry: A practical Guide for Applying Techniques to Real World Problems, Wiley-Interscience, New York, 2001.

[4] R. Srikanth, R. Srinivas, K. Bhanuprakash, S. Vivekananda, E.A. Syrstad, F. Tureček, J. Am. Chem. Soc. Mass Spectrom. 13 (2002) 250 (and references cited therein).

[5] S. Vivekananda, R. Srinivas, Int. J. Mass Spectrom. Ion Process. 171 (1997) 79.

[6] A.C. Chukwudebe, M.A. Hussain, P.C. Oloffs, J. Environ. Sci. Health B19 (6) (1984) 523.

[7] L.N. Heydorn, P.C. Burgers, P.J.A. Ruttink, J.K. Terlouw, in preparation.

[8] L.N. Heydorn, P.C. Burgers, P.J.A. Ruttink, J.K. Terlouw, Int. J. Mass Spectrom. Ion Process. (2002), in press.

[9] (a) J.K. Terlouw, H. Schwarz, Angew. Chem. Int. Ed. Engl. 26 (1987) 805;
(b) M.A. Trikoupis, J.K. Terlouw, P.C. Burgers, M. Peres, C. Lifshitz, J. Am. Soc. Mass Spectrom. 10 (1999) 869.

[10] (a) C. Furlani, M.V. Andreocci, J. Chem. Soc. (Dalton) (1972) 248;
(b) D.G. Hewitt, Aust. J. Chem. 32 (1979) 463;
(c) P.C. Crofts, I.S. Fox, J. Chem. Soc. (1958) 2995;
(d) Houben-Weyl, Methoden der Organischen Chemie, vol. XII/2, Georg Thieme Verlag, Stuttgart, 1964.

[11] H.F. van Garderen, P.J.A. Ruttink, P.C. Burgers, G.A. McGibbon, J.K. Terlouw, Int. J. Mass Spectrom. Ion Process. 121 (1992) 159.

[12] (a) J.A. Montgomery Jr., M.J. Frisch, J.W. Ochterski, G.A. Petersson, J. Chem. Phys. 110 (1999) 2822;
(b) J.A. Montgomery Jr., M.J. Frisch, J.W. Ochterski, G.A. Petersson, J. Chem. Phys. 112 (2000) 6532.

[13] L.N. Heydorn, Y. Ling, G. de Oliveira, J.M.L. Martin, Ch. Lifshitz, J.K. Terlouw, Zeitschrift für Physikalische Chemie 215 (2001) 141.

[14] M.J. Frisch, et al. Gaussian 98, Revision A.9, GAUSSIAN Inc., Pittsburgh, PA, 1998.

[15] S.G. Lias, J.E. Bartmess, J.F. Liebman, J.L. Holmes, R.D. Levin, W.G. Mallard, J. Phys. Chem. Ref. Data 17 (Suppl. 1) (1988) see also NIST Chemistry WebBook, http://webbook.nist.gov/chemistry/.

[16] NIST Chemistry WebBook, http://webbook.nist.gov/chemistry/.

[17] R. Flammang, V. Henrotte, P. Gerbaux, M.T. Nguyen, Eur. Mass Spectrom. 6 (2000) 3.

[18] (a) C.E.C.A. Hop, Ph.D. Thesis, University of Utrecht, 1988;
(b) C.E.C.A. Hop, J.L. Holmes, Org. Mass Spectrom. 26 (1991) 476.

[19] S. Beranová, C. Wesdemiotis, J. Am. Chem. Soc. Mass Spectrom. 5 (1994) 1093.